Article

Eliminating Non-uniform Smearing and Suppressing the Gibbs Effect on Reconstructed Images †

Valery Sizikov*, Aleksandra Dovgan, Aleksei Lavrov

Faculty of Software Engineering and Computer Technigue, ITMO University, Saint-Petersburg 197101, Russia

* Correspondence: sizikov2000@mail.ru

† This paper is an extended version of our report: Sizikov, V.; Dovgan, A.; Lavrov, A. "Suppressing the Gibbs Effect on Reconstructed Images" in the Majorov International Conference on Software Engineering and Computer Systems (MICSECS 2019), Saint-Petersburg, Russia, 12–13 December 2019.

Abstract. In this work, the problem is considered for eliminating a non-uniform rectilinear smearing of an image by mathematical and computer-based way, for example, a picture of several cars taken with a fixed camera and moving with different speeds. The problem is described by a set of 1-dimensional Fredholm integral equations (IEs) of the first kind of convolution type with a 1-dimensional point spread function (PSF) at uniform smearing and by a set of new 1-dimensional IEs of a general type (not convolution type) with a 2-dimensional PSF at non-uniform smearing. The problem is also described by one 2-dimensional IE of convolution type with a 2-dimensional PSF at uniform smearing and by a new 2-dimensional IE of a general type with a 4-dimensional PSF at non-uniform smearing. The problem for solving Fredholm IE of the first kind is ill-posed (unstable). Therefore, IEs of convolution type are solved by the Fourier transform (FT) method and Tikhonov's regularization (TR), and IEs of general type are solved by the quadrature/cubature and TR methods. Moreover, the magnitude of the image smear Δ is determined by the original "spectral method", which increases the accuracy of image restoration. It is shown that the use of a set of 1-dimensional IEs is preferable to one 2-dimensional IE in the case of non-uniform smearing. In the inverse problem (image restoration), the Gibbs effect (the effect of false waves) in the image may occur. It can be edge or inner. The edge effect is well suppressed by the proposed technique "diffusing the edges". In the case of an inner effect, it is eliminated with difficulty, but the image smearing itself plays the role of diffusing and suppresses the inner Gibbs effect to a large extent. It is shown (in the presence of impulse noise in an image) that the well-known Tukey median filter can distort the image itself, and the Gonzalez adaptive filter also distorts the image (but to a lesser extent). We propose a modified adaptive filter. A software package was developed in MatLab and illustrative calculations are performed.

Keywords: smeared image; non-uniform rectilinear smear; integral equations; spectral method; edge and inner Gibbs effects; MatLab

1. Introduction

Consider one of the actual problems of distorted images processing – the elimination of image smearing by mathematical and computer-based way ([1–7], et al.). Smearing may be due to the shift of the image recording device (photo camera, video camera, telescope, microscope), the mismatch of the movement of the observation object (the earth's surface, details on the conveyor) and the tracking

Peer-reviewed version available at Computers 2020, 9, 30; doi:10.3390/computers9020030

device or the movement of the object itself (patient in tomograph, animal, car, plane) for exposure time [4,7].

The problem of smear eliminating by a mathematical way consists of two tasks: a direct problem (computer smear modeling) and an inverse problem (smear eliminating by equations' solving) [7] (p. 106–109). However, the inverse problem is very sensitive to the accuracy of the knowledge of smear magnitude Δ (as shown, for example, in [8]), especially if the smear is variable, i.e. $\Delta = \Delta(x)$, where x is the coordinate along the smear [5,6]. In this paper, we develop the "spectral method" proposed in [7–9] and use it to determine the smear Δ and $\Delta(x)$.

In this paper, we focus on the rarely considered image smearing, which is rectilinear, but non-uniform when the camera or object moves during the exposure, as well as on various types of integral equations used in the inverse problem. We will give special attention to the Gibbs effect (the effect of false waves), which often appears on images [4,5,7].

The authors of several publications [1–4,7–9] et al. consider the variant of uniform rectilinear image smearing, as well as variant of arbitrary (non-uniform curvilinear) smearing using a "blind" deconvolution method [10] (p. 192) , [11,12], but less often consider an intermediate variant of non-uniform rectilinear smear [1,2,5,6], also an actual variant.

The main **goal** of this work is a comparative consideration of two variants of rectilinear image smearing (uniform and non-uniform) and suppression of the Gibbs effect, which reduces the restored image quality.

Example: a smeared image of movable objects (athletes-runners, animals, cars, planes) moving with different speeds, taken with a fixed camera. Note that a variant was considered in [1,2] when a camera (or object) moved during the exposure rectilinearly with a certain speed $v(t)$, where t is time. This variant is quite complicated, since it requires solving the nonlinear equation $\delta(t(x)) = x$ with respect to t, where $\delta(t) = \int_0^t v(t')dt'$ [6]. In this paper and in [5,6], the simpler variant of smear is considered: $\Delta = \Delta(x)$, where x is the coordinate along the smear.

However, there is no a way in [5,6] to determine the dependence $\Delta(x)$ from a smeared image. In this paper, we propose such a way ("divided spectra") based on the "spectral method".

The article is organized as follows. Section 2 describes the uniform rectilinear image smearing mathematically as the direct problem (integral calculation) and inverse problem (image restoration via solving a set of 1-dimensional IEs or one 2-dimensional IE by the FT and TR method). Section 3 describes the non-uniform rectilinear image smearing via solving by the method of quadrature/cubature and TR a set of 1-dimensional IEs or one 2-dimensional IE of general type (not convolution type). In section 4, an illustrative numerical example is given: 3 cars moving with the same smear Δ. The smear is determined by the spectral method. The results of image restoration by the FT and TR methods are presented. The question of restoration error is stated. In section 5, the results for example solving are presented in the case of various smeares of automobiles. A way of "divided spectra" for determining the dependence $\Delta(x)$ is proposed. Section 6 describes the impulse noise filtering and its influence on the image itself. A modified median filter for impulse noise suppressing is proposed. In all sections, we use the technique "diffusing the image edges" that we proposed for suppressing the Gibbs effect.

2. Mathematical description of uniform rectilinear smearing an image

Let us recall the well-known case of uniform smearing an image [4,7,9]. Consider the direct and inverse problems.

2.1. Direct problem

The direct problem of uniform rectilinear smearing an image is to calculate the integral [6]

$$g_y(x) = \frac{1}{\Delta}\int_x^{x+\Delta} w_y(\xi)\,d\xi, \tag{1}$$

where Δ = const is the smear magnitude; the axes x and ξ are directed along the smear, and the axis y is perpendicular to the smear (plays the role of a parameter); $w_y(\xi)$ is the given non-smeared image, and $g_y(x)$ is the calculated (modeled) smeared image in each y-line. In order to calculate g according to (1), we developed in MatLab the main program Autos.m and m-functions smearing.m [7] for an arbitrary smear angle θ and smear.m [5] for $\theta = 0$. In addition, the MatLab system has m-functions fspecial.m and imfilter.m for modeling g [10].

We notice that the description of the smearing problem by an integral (and, as a consequence, by an integral equation, see below) is the most adequate mathematical description of the image smearing process.

The following algorithm describes solving the direct problem according to [7] (pp. 116–118).

Algorithm 1. The direct problem of uniform rectilinear smearing an image

---

Input: exact (undistorted) image w

(1) Assignment of smear magnitude Δ and smear angle θ

(2) Turn of image w about angle θ and introduction of boundary conditions (BCs), truncation or diffusion of edges

(3) Calculation of the smeared image g line-by-line in the discrete form: $g_j(i) = \frac{1}{\Delta+1}\sum_{k=i}^{i+\Delta} w_j(k)$, $j = 1,2,\text{K}\,,m$, $i = 1,2,\text{K}\,,N$, where j and i are the numbers of rows and columns of turned image, and $N = n - \Delta$ when truncating and $N = n + \Delta$ when diffusing the image edges

(4) Inverse turn of the image g

Output: g

2.2. Inverse problem

The inverse (more important and complex) problem can be solved by *two approaches*.

In the *first approach*, in order to eliminate the smearing, we solve a set of 1-dimensional Fredholm integral equations (IEs) of the first kind of convolutional type (for each value of y) [6,7,9]:

$$\int_{-\infty}^{\infty} h(x-\xi)\,w_y(\xi)\,d\xi = g_y(x), \quad -\infty < x < \infty. \tag{2}$$

where

$$h(x) = \begin{cases} 1/\Delta, & -\Delta \le x \le 0, \\ 0, & \text{otherwise.} \end{cases} \tag{3}$$

Preprints (www.preprints.org) | NOT PEER-REVIEWED | Posted: 9 March 2020 doi:10.20944/preprints202003.0149.v1

Peer-reviewed version available at Computers 2020, 9, 30; doi:10.3390/computers9020030

The IE (2) is obtained from the relation (1); axes x and ξ are directed along the smear and axis y perpendicular to the smear; h is the kernel of IE mathematically, and the point spread function (PSF) physically and technically [3,4,7,11,13]. The function h, as a rule, is difference, or spatially invariant, which means that the smearing is uniform and the smear magnitude Δ is the same at all points of the image (Δ = const).

The problem of solving IE (2) is ill-posed (unstable) [14–17]. We use the stable Tikhonov regularization method (TRM, TR) with the Fourier transform (FT) [4,7,9,16,18]:

$$w_{\alpha y}(\xi) = \frac{1}{2\pi} \int_{-\infty}^{\infty} W_{\alpha y}(\omega)\, e^{-i\omega\xi}\, d\omega\,, \tag{4}$$

where

$$W_{\alpha y}(\omega) = \frac{H(-\omega)\, G_y(\omega)}{|H(\omega)|^2 + \alpha\, \omega^{2p}} \tag{5}$$

is the regularized Fourier spectrum (FS) of the solution; $H(\omega) = F(h(x))$ and $G_y(\omega) = F(g_y(x))$ are Fourier spectra of functions $h(x)$ and $g_y(x)$, where F is the sign of FT; $\alpha > 0$ is the regularization parameter; $p \geq 0$ is the regularization order (usually $p = 1$ or $p = 2$). Several ways have been developed for choosing the regularization parameter α: the discrepancy principle, the method of training examples, the selection method, etc. [2,7,14,17,18]. In order to calculate the reconstructed image using formulas (4), (5), we developed the m-function desmearingf.m [10]. In addition, the MatLab system has the m-function deconfreg.m [10].

The following algorithm describes the solution of inverse problem (the first approach).

Algorithm 2. The inverse problem of uniform rectilinear smearing (the first approach)

Input: smeared image $g(x, y)$, where x and y are directed horizontally and vertically respectively

(1) Calculating the Fourier spectrum $G(\omega_1, \omega_2) = F(g(x, y))$, where x is horizontally, and y vertically

(2) Determining the smear Δ and angle θ values from the Fourier spectrum (via spectral method)

(3) Calculating the PSF $h(x)$ according to (3), where x is directed along the smear and y is perpendicular to the smear

(4) Calculating the Fourier spectra $H(\omega) = F(h(x))$ and line-by-line $G_y(\omega) = F(g_y(x))$

(5) The choice of the regularization parameter α in some way

(6) Calculating line-by-line (for every y) the $W_{\alpha y}(\omega)$ – the regularized Fourier spectrum of desired solution $w_{\alpha y}(\xi)$ according to (5)

(7) Calculating line-by-line the restored image as the IFT: $w_{\alpha y}(\xi) = F^{-1}\left(W_{\alpha y}(\omega)\right)$ according to (4)

(8) Inverse turn of the image and obtaining $w(x, y)$, where x is horizontally, and y vertically

Output: $w(x, y)$

In the *second approach*, to eliminate the smearing (as well as defocusing), a 2-dimensional Fredholm integral equation of the first kind of convolution type is used (cf. (2)) [2,6,7]:

$$\int_{-\infty}^{\infty}\int_{-\infty}^{\infty} h(x-\xi, y-\eta)\, w(\xi,\eta)\, d\xi\, d\eta = g(x,y), \quad -\infty < x, y < \infty, \tag{6}$$

moreover, the x and ξ axes are directed horizontally, and y and η are directed vertically downward. PSF h is displayed on the plane (x, y) as a narrow strip [6], [7] (p. 112).

In this approach, the direct problem is calculated using the m-functions fspecial.m and imfilter.m [10]. And the solution of the 2-dimensional IE (6) (the inverse problem) by the TR method and the 2-dimensional FT is equal to $w_\alpha(x,y) = F^{-1}\left(W_\alpha(\omega_1,\omega_2)\right)$, where F^{-1} is the inverse Fourier transform (IFT), or

$$w_\alpha(x,y) = \frac{1}{4\pi^2}\int_{-\infty}^{\infty}\int_{-\infty}^{\infty} W_\alpha(\omega_1,\omega_2)\, e^{-i(\omega_1 x+\omega_2 y)}\, d\omega_1\, d\omega_2, \tag{7}$$

moreover $W_\alpha(\omega_1,\omega_2)$ is the regularized spectrum (2-dimensional FT) of the solution, equal to

$$W_\alpha(\omega_1,\omega_2) = \frac{H^*(\omega_1,\omega_2)G(\omega_1,\omega_2)}{|H(\omega_1,\omega_2)|^2 + \alpha(\omega_1^2+\omega_2^2)^p}, \tag{8}$$

where $H(\omega_1,\omega_2) = F(h(x,y))$, $G(\omega_1,\omega_2) = F(g(x,y))$. The MatLab contains the m-function deconvreg.m [10] for solving IE (6) by the TR and FT methods according to (7), (8).

The following algorithm describes the solution of inverse problem (the second approach).

Algorithm 3. The inverse problem of uniform rectilinear smearing (the second approach)

Input: smeared image $g(x, y)$, where x and y are directed horizontally and vertically

(1) Calculating the Fourier spectrum $G(\omega_1,\omega_2) = F(g(x,y))$

(2) Determining the smear magnitude Δ and the smear angle θ from the spectrum (via spectral method)

(3) Building the PSF $h(x, y)$ in the form of a strip of length Δ at an angle θ

(4) Calculating the Fourier spectrum $H(\omega_1,\omega_2) = F(h(x,y))$

(5) Choice of the regularization parameter α in some way and regularization order p

(6) Calculating the $W_\alpha(\omega_1,\omega_2)$ – the regularized Fourier spectrum of the solution according to (8)

(7) Computating the restored image in the form of IFT: $w_\alpha(x,y) = F^{-1}\left(W_\alpha(\omega_1,\omega_2)\right)$ according to (7)

Output: $w(x, y)$

We give the well-known formulas (1)–(8) in order to compare the various approaches below.

3. Mathematical description of non-uniform rectilinear smearing

Taking into account the formulas (1)–(8), we discribe non-uniform rectilinear smearing of image along the smear direction. Let us consider *two approaches*.

3.1. The first (time) approach [1,2,6]

In this approach, the speed of moving object (or camera) is assumed to be known as a function $v(t)$ of time $t \in [0, \tau]$, where τ is the exposure time. This approach was considered in detail in [6], and we consider the second, simpler approach.

3.2. The second (spatial) approach [5,6]

Suppose that we have determined a dependence $\Delta = \Delta(x)$ of the smear Δ on the x coordinate directed along the smear. This dependence may be determined from the smeared image in some way, for example, by the method of "blind" deconvolution [11] or by the spectral method [9] (see section 4).

3.2.1. The direct problem

In this case, the PSF h is not difference, or spatially invariant, and *the direct problem* is written in the form (cf. (1)):

$$g_y(x) = \frac{1}{\Delta(x)} \int_x^{x+\Delta(x)} w_y(\xi) d\xi \,. \tag{9}$$

To calculate $g_y(x)$ according to (9), we developed the m-function smear_n.m [5].

3.2.2. The inverse problem

The *inverse problem* in the case of the second approach is written in the form of a set of 1-dimensional Fredholm integral equations of the first kind of general type (not convolutional type) for each value of y [5,6]:

$$Aw_y \equiv \int_a^b h(x,\xi) w_y(\xi) d\xi = g_y(x), \quad c \le x \le d \,, \tag{10}$$

where A is integral operator; $[a,b]$ and $[c,d]$ are limits for ξ and x. The PSF h is written as

$$h(x,\xi) = \begin{cases} 1/\Delta(x), & x \le \xi \le x + \Delta(x), \\ 0, & \text{otherwise.} \end{cases} \tag{11}$$

The FT method cannot be applied for solving IE (10), since the IE (10) is not a convolutional type equation, but the *quadrature method* can be applied, which reduces the IE (10) to a system of linear algebraic equations (SLAE) for each y [7] (p. 126):

$$Aw_y = g_y \,, \tag{12}$$

where A is the matrix, associated with h (the same for all y-rows), w_y is the desired vector, g_y is the right-hand side of the SLAE. A stable solution of SLAE (12) is provided by the Tikhonov regularization method (TRM) [7]:

$$(\alpha I + A^T A) w_{y\alpha} = A^T g_y \,, \tag{13}$$

where $\alpha > 0$ is the regularization parameter (about the α choice method see below Figure 5), I is the identity matrix, A^T is the transposed matrix, and $w_{y\alpha}$ is the regularized solution in each y-row, equal to

$$w_{y\alpha} = (\alpha I + A^T A)^{-1} A^T g_y \,. \tag{14}$$

In order to realize the formulas (10)–(14) on a computer, we developed the m-function desmearq_n.m. Note that the quadrature method with Tikhonov's regularization (TR) according to

(13), (14) can be used also for solving IE of convolution type (2) with the PSF (3), i.e. for uniform smearing. For that, we developed the m-function desmearq.m.

The *inverse problem* in the framework of the *second approach* can be written also in the form of a 2-dimensional Fredholm IE of the first kind of general type [18] (cf. (6)):

$$Aw \equiv \int_a^b \int_c^d h(x,\xi,y,\eta)\, w(\xi,\eta)\, d\xi\, d\eta = g(x,y), \quad a \le x \le b, \quad c \le y \le d\,. \tag{15}$$

Integral equation (15) can be solved by the *quadrature method* (more precisely, *cubature method*) (cf. [18, p. 167]).

According to this method, each of the integrals in (15) is replaced by a finite sum on discrete grids of nodes in x, ξ, y, η and we obtain a SLAE with a 4-dimensional matrix A, a 2-dimensional right-hand side g and a 2-dimensional desired function w. To solve such a SLAE by known methods (Gauss, et al.), it is necessary to transform the 4-dimensional matrix A into a 2-dimensional one, to transform the 2-dimensional right-hand side g into a 1-dimensional one, to solve such a SLAE, and to transform the resulting 1-dimensional solution w into a 2-dimensional one.

The solution of a 2-dimensional IE by the cubature method took place, for example, in [18] (p. 168), however, with a small matrix 11×11×7×7, i.e. $11^2 \times 7^2$. If an image g has real dimensions, e.g., 400×400 pixels, then it is necessary to solve a SLAE with a 2-dimensional matrix of size $400^2 \times 400^2$, i.e. a matrix of gigantic size 160000×160000, which is implemented with difficulty even on powerful computers. We see that the cubature method for solving IE (15) is a cumbersome method and its application to restore a non-uniform smeared image is complex.

It is possible to use the iteration methods of Jacobi, Landweber, Friedman, Bakushinsky, et al. [2,15,18] for solving 2-dimensional IE (15). These methods usually do not use giant arrays, however, they require a successful initial approximation for w, the number of iterations (playing the role of a regularization parameter), etc.

As a result, we conclude that the most effective technique in the case of non-uniform smearing is the technique (10)–(14), based on line-by-line image processing by solving 1-dimensional IE (10) and SLAE (12) with 2-dimensional matrix in each y-line and on the subsequent combination of row-wise solutions into a single 2-dimensional image.

The following algorithm describes the line-by-line solution of inverse problem.

Algorithm 4. The inverse problem of a row-wise non-uniform rectilinear smear

---

Input: image $g(x, y)$ smeared non-uniformly along x

(1) Presentation of a 2-dimensional image $g(x, y)$ as a set of 1-dimensional images $g_y(x)$

(2) Determining the non-uniform smear $\Delta(x)$ from the spectrum (via spectral method)
(3) Calculating the PSF $h(x,\xi)$ according to (11)

(4) Writing matrix A and vectors g_y of a system of linear algebraic equations (SLAE)

(5) Choice of the regularization parameter α in some way
(6) Solving the regularized SLAE (13) in each y-row

(7) Obtaining a regularized solution $w_{y\alpha}$ according to (14)

(8) Forming image $w_\alpha(x, y)$ from a set of row-wise solutions $w_{y\alpha}$

Output: $w_\alpha(x, y)$

---

4. Illustrative example

The following *numerical example* is solved. Figure 1 shows grayscale (gray) initial image J of three cars (file Autos.png).

Image J has intensities from 0 to 255, which causes inconvenience in filtering impulse noise, which has values 0 and 255 (see details in section 6).

To avoid this inconvenience, we replaced the intensities 0 and 255 of the image J with the values 1 and 254. We obtained the image I with intensities from 1 to 254.

We use the image I, 143×1307 pixels for further processing,. Note that the driver's head is visible in the left car, which (along with the wheels) will be one of the reference points in image processing.

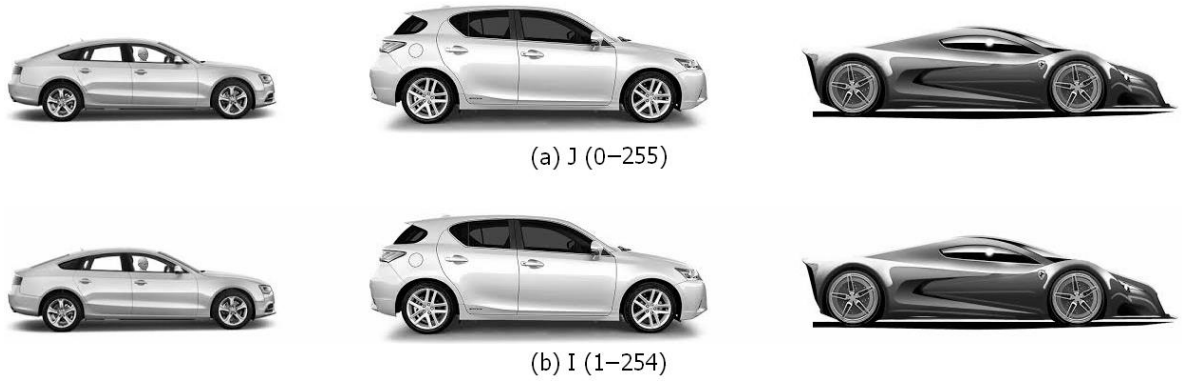

Figure 1. Initial (undistorted) image of stationary cars, 143×1307 pixels. (a) Image J with intensities from 0 to 255; (b) image I with intensities from 1 to 254.

4.1. Uniform smearing of image using Boundary Conditions

Further, we assume that the cars move at the same speed and therefore give the same smear in the image: Δ = const = 20 pixels or the cars are stationary, but the camera moves uniformly during the exposure. Image I is smeared horizontally according to (1) using the head program Autos.m and the m-functions fspecial.m and imfilter.m at Δ = 20. Furthermore, a "boundary condition" is used in the m-function imfilter.m with the option 'circular'. Figure 2a presents a smeared image (see smeared head of driver and smeared wheels).

Preprints (www.preprints.org) | NOT PEER-REVIEWED | Posted: 9 March 2020 doi:10.20944/preprints202003.0149.v1

Peer-reviewed version available at Computers 2020, 9, 30; doi:10.3390/computers9020030

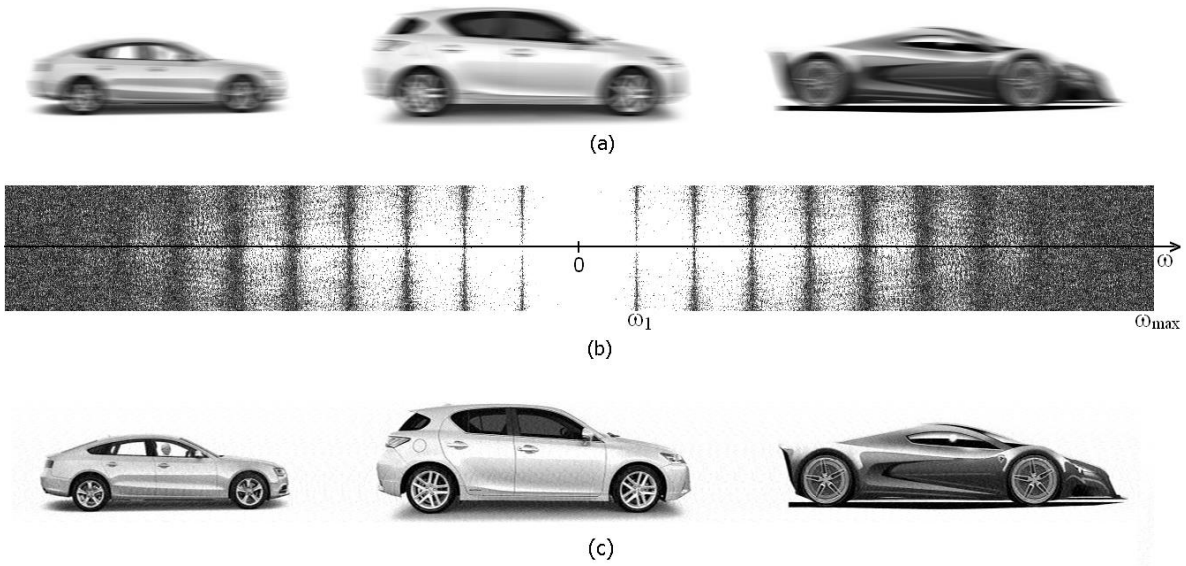

Figure 2. Image 143×1307 smeared uniformly (a); 2-dimensional centered FT (spectrum) in modulus of image 143×1307 (b); image 143×1307 restored by the FT and TR method (c).

In order to restore the image by solving inverse problem, it is necessary to know the angle θ and the smear Δ. It is possible to estimate these parameters visually, but only with an error, or it is impossible to estimate them at all. And, as we showed in [8, 19], even an error of θ in 1–2 degree and an error of Δ in 1–2 pixel lead to a significant error (~ 10%) in image restoration even by Tikhonov regularization or Wiener parametric filtering method.

In [7–9,19], we developed the so-called "spectral method", which allows to determine the distortion type (smearing, defocusing, etc.) and estimate the distortion parameters based on the Fourier transform (Fourier spectrum) of the distorted image. Let us use the spectral method. Figure 2b presents the Fourier spectrum in modulus $|G(\omega)|$ of distorted image in Figure 2a. As follows from Figure 2b, the image in Figure 2a is uniformly smeared (this follows from a theory and a large number of Fourier spectra of smeared, defocused, and other images [3,6–9,19–21]). In addition, one can estimate the smear magnitude Δ by the formula

$$\Delta = 2\frac{\omega_{\max}}{\omega_1}, \tag{16}$$

where ω_1 and $\omega_{\max}$ are the first and last zeros of the transfer function $H(\omega) = F(h(x))$ (see the details in [9]). For several measures in Figure 2b, we get on average $\Delta = 20.08 \pm 0.05$ pixels, which is close to the exact value of $\Delta = 20$. Using the value of Δ, we restored the cars' image (Figure 2c) by the FT and TR method according to (6)–(8) using m-function deconvreg.m with $\alpha = 10^{-4.2}$ (α value is chosen by the minimum of curve 1 in Figure 5); relative error is $\sigma_{\text{rel}} = 0.0359$ (according to (17)).

4.2. Uniform smearing of image with truncation

The Boundary Conditions (BCs) [10,22] used in m-function imfilter.m are an artificial technique intended for determining the intensities of an undistorted image outside its edges. We proposed [7,23] instead of BCs the technique of image truncation, which does not require extraboundary data. Figure 3a presents the image 143×1267 smeared uniformly with a truncation modeled using m-function smear.m (with the option 'truncation'), and Figure 3b presents the image restored by the FT and TR method using m-function desmearq.m with $\alpha = 10^{-1.2}$ and $\sigma_{\text{rel}} = 0.269$. We see the

Peer-reviewed version available at Computers 2020, 9, 30; doi:10.3390/computers9020030

significant edge and smaller inner Gibbs effects in Figure 3b. This is due to a sharp jump of intensity on the edges of image if it is truncated. Nevertheless, the truncation technique can be effective in the case of a finite image (a space object on a dark background [7] (p. 105), [22], etc.).

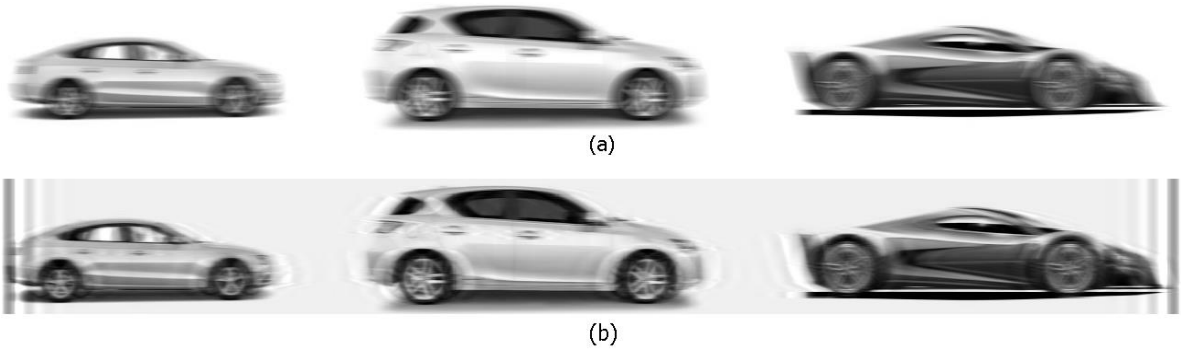

Figure 3. Image smeared uniformly with truncation (a); restored image (b).

4.3. Uniform smearing of image with diffusing the image edges

In [7,23], we proposed a way of diffusing the smeared image edges to suppress the edge Gibbs effect. The Gibbs effect (distortion of the "ringing" type) is due to a stepwise change in intensity of the Heaviside step function type. Mathematically, the Gibbs effect can be explained by the fact that the FT of the step function gives the sinc function with side fluctuations. In order to suppress these false fluctuations, it was proposed in [10] (p. 185) to use the m-function edgetaper.m, which diffuses the image edges. However, modeling has shown that this function does not sufficiently diffuse the edges, and the foregoing Algorithm 1 is more effective. At the same time, the inner Gibbs effect is eliminated more difficult, but the image smearing itself reduces the intensity jump and reduces the inner Gibbs effect (see middle of Figure 3b).

The technique of smearing the image edges resembles the edges' smoothing of the transfer function $H(\omega)$, as well as the image smoothing via the Butterworth low-frequancy filter [4] (p. 265–267), [10] (p. 143), etc. However, these filters make an enhancement of edges' smoothing in the frequency domain, and our technique realizes the edges' diffussing of the image itself immediately, which leads to a greater suppression of the Gibbs effect.

The diffusing of edges leads to a smooth decrease of intensity on the smeared image edges and to suppressing the Gibbs effect on restored image. Figure 4a presents the uniformly smeared image with the addition of diffusing its edges using m-function smear.m (with the option 'diffusion'). Figure 4b presents the result of cars' image restoration by the FT and TR method according to (12)–(14) using the m-function desmearq.m. We see that the introduction of diffusing the edges leads to the image restoration without the Gibbs effect and to almost exact restoration.

Preprints (www.preprints.org) | NOT PEER-REVIEWED | Posted: 9 March 2020 doi:10.20944/preprints202003.0149.v1

Peer-reviewed version available at Computers 2020, 9, 30; doi:10.3390/computers9020030

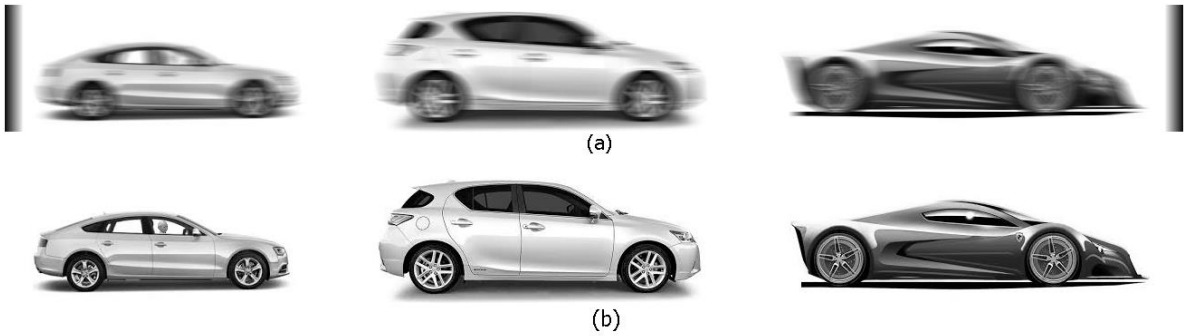

Figure 4. Image smeared uniformly with diffusing the edges (option 'diffusion'). a – smeared image 143×1327 (Δ = 20 pixels); b – restored image 143×1307 by TR method ($\alpha = 10^{-8}$), relative error of restoration $\sigma_{rel} \approx 0$.

4.4. Error estimation of image restoration

In order to estimate numerically the restoration quality and choose the regularization parameter α, we propose a formula for calculating relative error in the form of the standard deviation of the calculated image $\tilde{w}_\alpha$ from the exact image $\overline{w}$ [9]:

$$\sigma_{rel}(\alpha) = \frac{\| \tilde{w}_\alpha - \overline{w} \|_{L_2}}{\| \overline{w} \|_{L_2}} = \sqrt{\sum_{j=1}^{M}\sum_{i=1}^{N}\left(\tilde{w}_{\alpha ji} - \overline{w}_{ji}\right)^2} \Big/ \sqrt{\sum_{j=1}^{M}\sum_{i=1}^{N}\overline{w}_{ji}^2}\,, \qquad (17)$$

where M is the number of rows and N is the number of columns in the image. Such an expression for the image error can be used only in the case of model image processing when $\overline{w}$ is known (e.g., the image in Figure 1b). Figure 5 presents the curves $\sigma_{rel}(\alpha)$ for different variants of solutions. One can choose the value of α from the minima of these curves.

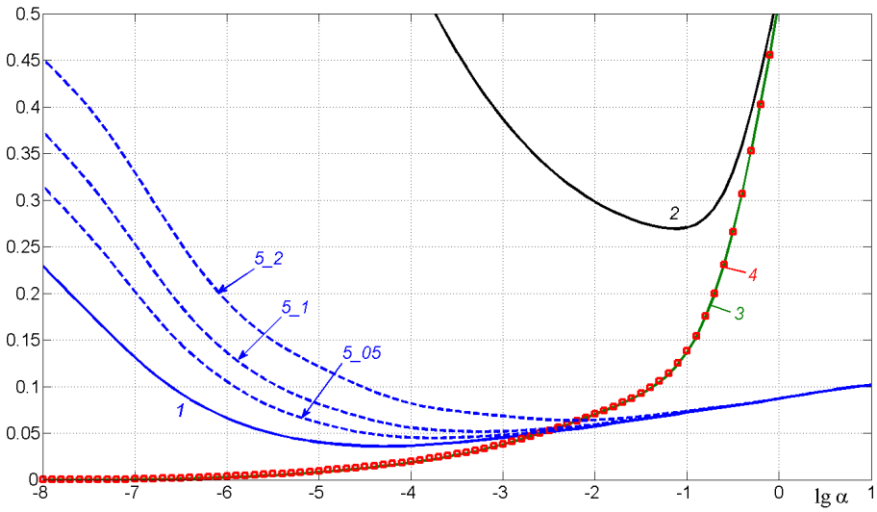

Figure 5. The relative error of image restoration $\sigma_{rel}(\alpha)$. *1* – FT and TR method (see Fig. 2c); *2* – FT and TR method with truncation (Fig. 3b); *3* – FT and TR method with diffused edges (Fig. 4b); *4* – quadrature and TR method with diffusing and division (Fig. 9); *5* – FT and TR method with noise, d = 0.005, 0.01, 0.02 (Fig. 10e).

One can also use the following expression for restoration error:

$$\mathrm{PSNR} = 10\lg\left(\overline{w}_{\max} MN \Big/ \|w - \overline{w}\|_{L_2}^2\right), \qquad (18)$$

Peer-reviewed version available at Computers 2020, 9, 30; doi:10.3390/computers9020030

where PSNR is the so-called peak signal-to-noise ratio, used widely in engineering, acoustics, etc. However, formula (17) is more convenient and obvious for image processing. Indeed, if, for example, the error according to (17) equals $\sigma_{rel} = 0.035$, then this means that the restoration error is 3.5%, and this value does not depend on the system of units w. Convenient and clear! And if we use the formula (18) and get an error, for example, 8 dB, then it is difficult to judge whether this is a large or small error in image restoration.

5. Direct and inverse problems of non-uniform smearing of image

The next step is *non-uniform smearing of an image*. We believe that the cars move with different speeds and therefore they have different smears on the image, for example, $\Delta = \Delta_1 = 15$ pixels for the left car, $\Delta = \Delta_2 = 20$ pixels for the middle car and $\Delta = \Delta_3 = 25$ pixels for the right car.

As a result, smear $\Delta(x)$ is a piecewise constant function:

$$\text{if (i<=360) } \Delta=15\text{; elseif (i<=820) } \Delta=20\text{; else } \Delta=25; \quad (19)$$

where i = 1 ... 1307 is the number of discrete reading along x.

Figure 6 shows an image smeared non-uniformly according to (9) and (19) with diffusing the edges for suppressing the Gibbs edge effect using m-function smear_n.

Figure 6. Image smeared non-uniformly with diffusing the edges.

In order to solve the inverse problem of image restoration, one needs to know the dependence (19) $\Delta(x)$ of the smear on x. However, we usually do not know this dependence in practice, or we can visually estimate it from Figure 6 only approximately. To determine $\Delta(x)$, we use the spectral method, as in Figure 2b. Figure 7 presents the Fourier spectrum in modulus $|G(\omega)|$ of distorted image $g(x, y)$ in Figure 6.

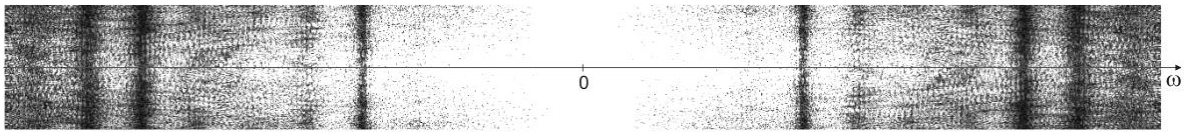

Figure 7. FT (Fourier spectrum) in modulus of non-uniformly smeared image in Fig. 6.

However, Figure 7 shows that the spectrum is the sum of three spectra and this creates difficulties with the definition of Δ_1, Δ_2 and Δ_3. We propose a way that we will call the "way of divided spectra".

5.1. The way of divided spectra

Let us divide the original piecewise-uniform smeared image in Figure 6 into 3 parts, for example, g1(:,22:344); g2(:,400:800), g3(:,854:1293). To perform such a division is not difficult. Figures 8abc present the divided parts g1, g2, g3 of the image in Figure 6.

Preprints (www.preprints.org) | NOT PEER-REVIEWED | Posted: 9 March 2020 doi:10.20944/preprints202003.0149.v1

Peer-reviewed version available at Computers 2020, 9, 30; doi:10.3390/computers9020030

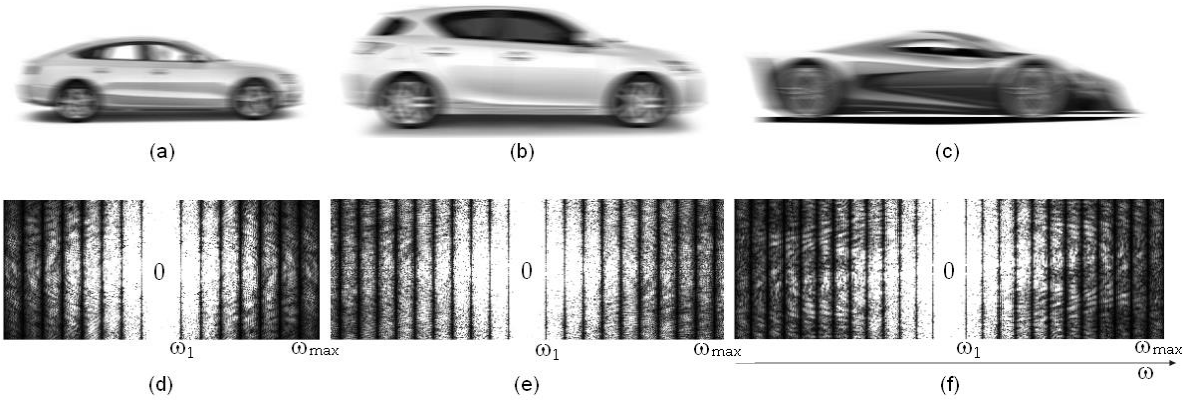

Figure 8. Divided parts of image (a,b,c); divided spectra in modulus (d,e,f).

Next, we calculate the FT (spectrum) in modulus |G| for each part of the image (Figure 8def, cf. Figure 2b). From the spectra, we determine the smears' magnitudes by the formula (16) and obtain (for several measures): $\Delta_1 = 14.95 \pm 0.40$, $\Delta_2 = 20.42 \pm 0.50$, $\Delta_3 = 24.99 \pm 0.60$ or rounded to integer values: $\Delta_1 = 15$, $\Delta_2 = 20$, $\Delta_3 = 25$.

Now, having determined rather accurately the divided smears Δ_1, Δ_2, Δ_3, and hence the dependence $\Delta(x)$, we solve the inverse problem of restorating a single (without division) image according to (10)–(14), namely, by the quadrature method with Tikhonov's regularization. Figure 9 presents the result of image restoration using the developed m-function desmearq_n.m. The image was restored almost accurately and without the Gibbs effect.

Figure 9. Restored single image 143×1307, $\sigma_{rel} \approx 0$ (see curve 4 in Fig. 5).

6. Noise accounting

In the above results, we did not take into account the influence of noise, therefore, we obtained clear restored images in Figures 2, 4, 9. Let us consider the influence of noise on the results of image processing for an example of impulse noise with intensities 0 and 255 [10,24,25].

In the Tukey median filter [4,7,24,25] (m-function medfilt2.m), a small window slides over the noisy image and at each position of the window, the intensity of center point of the window I_0 is replaced by the median intensity I_m. As a result, noise with intensities $I_n = 0$ and 255 is eliminated, but the image itself may be distorted, because, firstly, I_m can be different from I_0 and, secondly, I_0 can be equal to 0 or 255.

In [4] (p. 360) and [10] (p. 178), an adaptive median filter (a Gonzalez filter) was proposed (m-function adpmedian.m), according to which I_0 is replaced by I_m only when $I_0 = 0$ or 255, i.e. the central point is impulse. However, the Gonzalez filter can also distort the image itself when $I_0 = 0$ or 255, but the center point is not an impulse, but is the point of the image itself.

We propose a filter that we call a *modified median filter* (m-function modmed.m). According to this filter, it is supposed that the original noise-free image has no points with intensity 0 or 255, i.e. $0 < I_0 < 255$, and replacing I_0 with I_m in a noisy image is performed only when $I_0 = 0$ or 255, i.e.

when the center point is really an impulse, as in the Gonzalez filter. If the noise-free image has points with intensities 0 or 255, then it is proposed to replace $I_0 =$ 0 or 255 with $I_0 =$ 1 or 254 in the noise-free image (as in Figure 1).

The following algorithm describes the operations of the modified median filter.

Algorithm 5. Noise eliminating by the modified median filter

Input: g – image noisy by bipolar impulse noise

(1) Initial (noise -free) image of size M×N

(2) Correction of w: for j = 1:M for i = 1:N if w(j,i)=0 then w(j,i)=1; if w(j,i)=255 then w(j,i)=254;

(3) Noising image w by impulse noise and obtaining image g

(4) Presentation of sliding window of size m×n (default 3×3)

(5) Tukey's filter (median intensity at each point): fmed = medfilt2(g,[m n]);

(6) Initial approximation of filtered image: f = g;

(7) Noise eliminating: for j = 1:M for i = 1:N if g(j,i)=0 or g(j,i)=255 then f(j,i) = fmed(j,i);

(replacement only if the point (j,i) is an impulse)

Output: f – image filtered by modified median filter

Figure 10a presents the image taken from Figure 2a and uniformly smeared (Δ = const = 20 pixels). Figure 10b presents an image that is smeared and slightly noisy by impulse noise (the share of noising is d = 0.005, i.e. 0.5%). Figure 10c shows an image cleared from noise by the modified median filter (m-function modmed.m). The elimination of noise seemed to be successful, but the FT (spectrum) in modulus in Figure 10d of image from Figure 10c is insufficiently clear, unlike the clear spectrum in Figure 2b. And, as a result, eliminating the image smear in Figure 10c by the FT and TR method using the m-function deconvreg.m gives an insufficiently accurate result (Figure 10e, $\alpha = 10^{-3.7}$, $\sigma_{rel} = 0.0448$, see curve 5_05 in Figure 5), besides with a weak Gibbs effect.

Preprints (www.preprints.org) | NOT PEER-REVIEWED | Posted: 9 March 2020 doi:10.20944/preprints202003.0149.v1

Peer-reviewed version available at Computers 2020, 9, 30; doi:10.3390/computers9020030

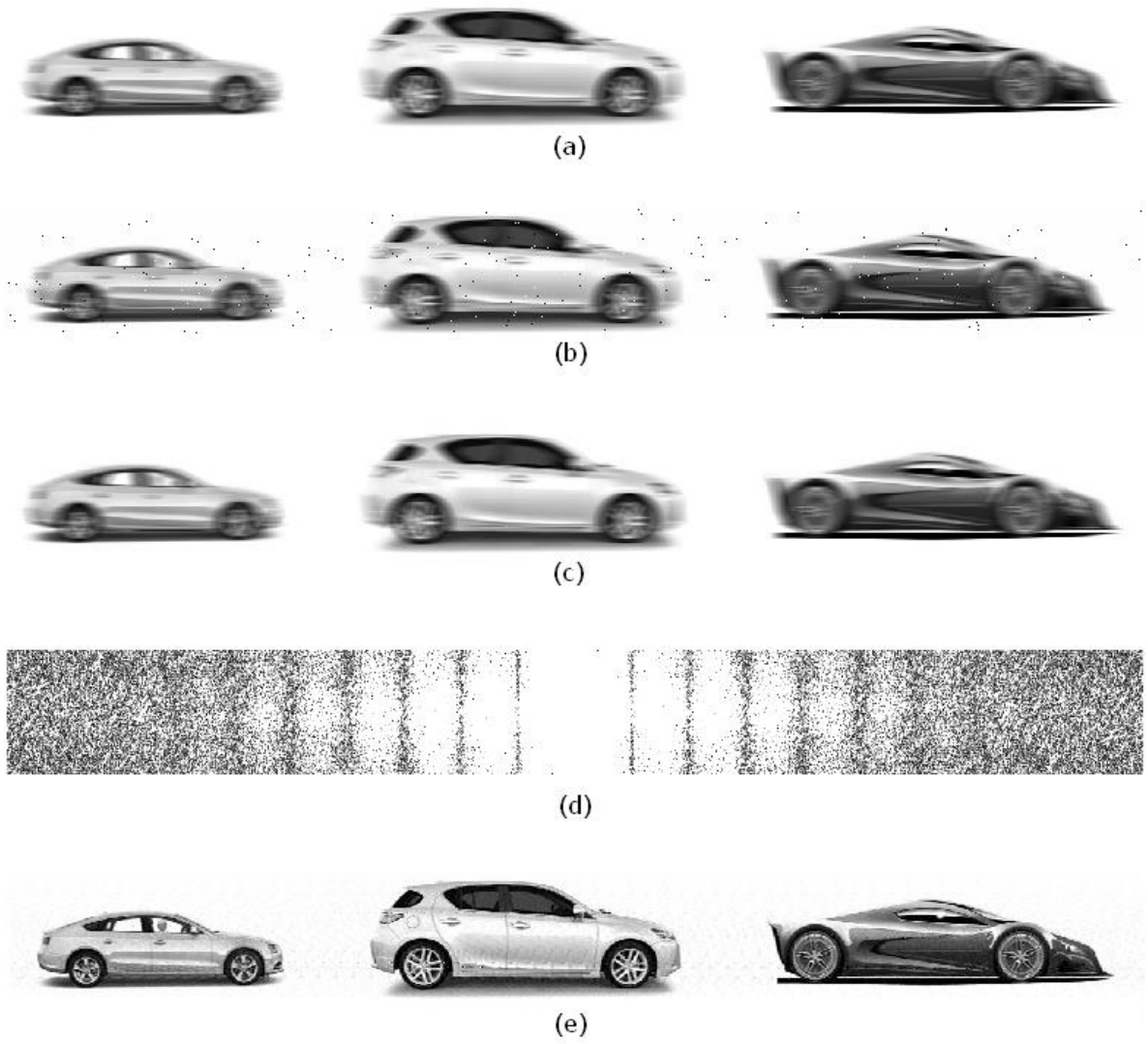

Figure 10. Accounting the noise influence. (a) Image smeared uniformly; (b) image smeared uniformly and noisy (d = 0.005); (c) image filtered from noise using modmed.m; (d) FT (spectrum) in modulus; (e) image restored by the FT and TR method.

Note that the intensities in the image in Figure 10a were artificially put equal from 1 to 254, as the modified median filter requires.

We also note that the impulse noise level (the share of noising) was put equal to d = 0.005, 0.01 and 0.02 (see Figures 10 and 5) in order to determine the dependence of the modified median filter error on the noise level. We see from a comparison of the images in Figures 10a and 10c that this filter well eliminates noise, but slightly distorts the image itself (Figure 10c) and this leads to a noticeable distortion of the spectrum (Figure 10d) and the restored image (Figure 10e).

This means that the Tukey median filter has an error in restoring the center point of a sliding window. If we pass through medfilt2.m even a noise-free image, for example, the smeared image S1 in Figure 10a, we get the image Sf1 = medfilt2(S1, [3 3], 'symmetric'); which differents from S1 on 2.4%, i.e. the Tukey median filter distorts an image even in the noise absence. And since both the Gonzalez filter and our modified filter refer to the Tukey filter, they also distort an image (cf. Figures 10a and 10c). The relative error of the Tukey filter is $\sigma_{rel} = 0.0244$, the Gonzalez filter is $\sigma_{rel} = 0.0135$, and the modified filter is $\sigma_{rel} = 0.0017$ at noise d = 0.005.

Peer-reviewed version available at Computers 2020, 9, 30; doi:10.3390/computers9020030

7. Conclusion

In this paper, we describe a technique of restoring the smeared images in the case when the smearing is rectilinear horizontal, but non-uniform, in particular, piecewise uniform (example: the cars on a road). It is proposed to solve a set of 1-dimensional integral equations (IEs) (the first approach) or one 2-dimensional IE (the second approach). In both approaches, the equations are not convolution type IEs, therefore, they are solved by the quadrature/cubature method with Tikhonov's regularization. It is shown that the first approach is more preferable than the second approach. Numerical examples confirm this. We developed programs in the MatLab system and performed illustrative calculations.

In order to determine the image smear of a variable quantity $\Delta = \Delta(x)$, we proposed a new modification of the "spectral method" (the "way of divided spectra"), which increases the accuracy of image restoration.

It is also shown that to improve the quality of image restoration, the image edges' diffusing should be used for suppressing the Gibbs edge effect (a false wave effect). The Gibbs effect may also be inner. In this case, it is suppressed by image smearing, which reduces the jump in intensities.

We proposed a new filter for eliminating impulse noise in the image – a modified median filter that suppresses noise but almost does not distort the image.

The technique can be used in practice for restoring grouped images of several objects (people, planes, cars) moving with different speeds and therefore receiving different smears Δ in the image during exposure by a fixed camera.

Author Contributions: conceptualization, V.S.; methodology, V.S. and A.D.; software, V.S.; formal analysis, V.S. and A.L.; data curation, V.S. and A.D.; writing—original draft preparation, V.S. and A.D.; writing—review and editing, V.S., A.D. and A.L.; visualization, V.S. and A.D.

Funding: This research was funded by MFCTC ITMO (Project № 619296).

Conflicts of Interest: The authors declare no conflict of interest.

References

1. Tikhonov, A.N.; Goncharsky, A.V.; Stepanov, V.V. *Inverse Problems of Photoimages Processing*. In: Ill-Posed Problems in Natural Science. Editor Tikhonov, A.N., Editor Goncharsky, A.V, Eds.; MSU Publ.: Moscow, Russia, 1987; pp. 185–195.
2. Bakushinsky, A.; Goncharsky, A. *Ill-posed Problems: Theory and Applications;* Kluwer Academic Publishers: Dordrecht, 1994; 199 pp. doi: 10.1007/978-94-011-1026-6.
3. Gruzman, I.S.; Kirichuk, V.S.; Kosykh, V.P.; Peretyagin, G.I.; Spektor, A.A. *Digital Image Processing in Information Systems*; NSTU Publ.: Novosibirsk, Russia, 2002; 352 pp.
4. Gonzalez, R.C.; Woods, R.E. *Digital Image Processing*, 2nd ed.; Prentice Hall, Upper Saddle River: NJ, USA, 2002; 797 pp.
5. Sizikov, V.; Dovgan, A. Reconstruction of images smeared uniformly and non-uniformly. *CEUR Workshop Proceedings* **2019**, 2344, paper2.pdf. 11 pp.
6. Sizikov, V.S.; Dovgan, A.N., Tsepeleva, A.D. Reconstruction of images smeared non-uniformly. *J. Optical Technology* **2020**, 87, 2, 1–8. doi: 10.1364/JOT.87.000095.
7. Sizikov, V.S. Direct and Inverse Problems of Image Restoration, Spectroscopy and Tomography with MatLab; Lan' Publ.: St. Petersburg, Russia, 2017; 412 pp.
8. Sizikov, V.S. Spectral method for estimating the point-spread function in the task of eliminating image distortions. *J. Optical Technology* **2017**, 84, 2, 95–101. doi: 10.1364/JOT.84.000095.
9. Sizikov, V.S.; Stepanov, A.V.; Mezhenin, A.V.; Burlov, D.I.; Éksemplyarov, R.A. Determining image-distortion parameters by spectral means when processing pictures of the earth's surface obtained from satellites and aircraft. *J. Optical Technology* **2018**, 85, 4, 203–210. doi: 10.1364/JOT.85.000203.
10. Gonzalez, R.C.; Woods, R.E.; Eddins, S.L. *Digital Image Processing using MATLAB*; Prentice Hall, Upper Saddle River: NJ, USA, 2004. 302 pp.
11. Fergus, R.; Singh, B.; Hertzmann, A.; Roweis, S.T.; Freeman, W. Removing camera shake from a single photograph. *ACM Trans. Graphics* **2006**, 25, 3, 787–794. doi: 10.1145/1141911.1141956.
12. Cho, S.; Lee, S. Fast motion deblurring. *ACM Trans. Graphics* **2009,** 28, 5, article no. 145.
13. Velho, L.; Frery, A.C.; Gomes, J. *Image Processing for Computer and Vision Graphics,* 2nd ed.; Springer-Verlag: London, 2009. 476 pp. doi: 10.1007/978-1-84800-193-0.
14. Tikhonov, A.N.; Arsenin, V.Ya. *Solutions of Ill-Posed Problems*; Winston: Washington, USA, 1977.
15. Engl, H.; Hanke, M.; Neubauer, A. *Regularization of Inverse Problems*; Kluwer: Dordrecht, 1996. 328 pp.
16. Petrov, Yu.P.; Sizikov, V.S. *Well-Posed, Ill-Posed, and Intermediate Problems with Applications*; Publisher VSP: Leiden, Netherlands, 2005. 234 pp.
17. Hansen, P.C. *Discrete Inverse Problems: Insight and Algoritms;* SIAM: Philadelphia, USA, 2010. 213 pp.
18. Verlan', A.F.; Sizikov, V.S. *Integral Equations: Methods, Algorithms, Programs*; Naukova Dumka: Kiev, Ukraine, 1986. 544 pp.
19. Sizikov, V.S. Estimating the point-spread function from the spectrum of a distorted tomographic image. *J. Optical Technology* **2015**, 82, 10, 655–658. doi: 10.1364/JOT.82.000655.
20. Bates, R.H.T.; McDonnell, M.J. *Image Restoration and Reconstruction*; Oxford U. Press: Oxford, 1986. 320 pp.
21. Jähne, B. *Digital Image Processing*; Springer: Berlin, 2005. 549 pp. doi: 10.1007/3-540-27563-0.
22. Nagy, J.G.; Palmer, K.; Perrone, L. Iterative methods for image deblurring: A Matlab object-oriented approach. *Numerical Algorithms* **2004**, 36**,** 1**,** 73–93. doi: 10.1023/B:NUMA.0000027762.08431.64.
23. Sizikov, B.C. The truncation – blurring – rotation technique for reconstructing distorted images. *J. Optical Technology* **2011**, 78, 5, 298–304. doi: 10.1364/JOT.78.000298.
24. Lim, J.S. *Two-dimensional Signal and Image Processing;* Prentice Hall PTR: NJ, USA, 1990. 694 pp.
25. D'yakonov, V.; Abramenkova, I. *MATLAB: Signal and Image Processing*; Piter: St. Petersburg, Russia, 2002. 608 pp.

.